Arabian Journal of Chemistry (2016) xxx, xxx–xxx

King Saud University

Arabian Journal of Chemistry

www.ksu.edu.sa
www.sciencedirect.com

ORIGINAL ARTICLE

Anti-*Helicobacter pylori*, cytotoxicity and catalytic activity of biosynthesized gold nanoparticles: Multifaceted application

V. Gopinath [a,b,*], S. Priyadarshini [a], D. MubarakAli [c,d], Mun Fai Loke [a], N. Thajuddin [d,e], Naiyf S. Alharbi [e], Tejabhiram Yadavalli [f], M. Alagiri [g], Jamuuna Vadivelu [a]

[a] *Department of Medical Microbiology, Faculty of Medicine, University of Malaya, Kuala Lumpur 50603, Malaysia*
[b] *Department of Biotechnology, SRM University, Kattankulathur, 603 203 Tamil Nadu, India*
[c] *Division of Bioengineering, Incheon National University, Incheon 406 772, Republic of Korea*
[d] *National Respository for Microalgae and Cyanobacteria-Freshwater, Department of Microbiology, Bharathidasan University, Tiruchirappalli 620 024, India*
[e] *Department of Botany and Microbiology, King Saud University, Saudi Arabia*
[f] *Nanotechnology Research Center, SRM University, Kattankulathur 603 203, India*
[g] *Center for Material science and Nanodevices, Department of Physics and Nanotechnology, SRM University, Kattankulathur, 603 203 Tamil Nadu, India*

Received 23 November 2015; accepted 6 February 2016

KEYWORDS

Biosynthesis;
Tribulus terrestris;
Gold nanoparticles;
Cell viability;
Anti-*Helicobacter pylori*

Abstract An unpretentious way to synthesize different sized gold nanoparticles (GNPs) using the dried fruit extract of *Tribulus terrestris* has been investigated. GNPs were formed due to the reduction of chloroauric acid ($HAuCl_4$) treated with the *T. terrestris* fruit extract. Formation of GNPs was periodically characterized by UV–Vis spectroscopy. IR spectrum revealed that phytochemicals in the extract played a key role in GNPs synthesis and stability. An anisotropic structure of GNPs with average sizes of 7 nm (GNP7) and 55 nm (GNP55) uses 1 and 2 mM $HAuCl_4$. The biogenic GNP showed a size dependent anti-*Helicobacter pylori* activity against multidrug resistant *H. pylori* strains. Furthermore, biogenic GNPs possess an excellent catalytic activity for the reduction of a toxic, *p*-nitroaniline to *p*-phenylenediamine as non-toxic by-product. Interestingly, *In vitro* cell

* Corresponding author at: Department of Medical Microbiology, Faculty of Medicine, University of Malaya, Kuala Lumpur 50603, Malaysia. Tel.: +60 12 9678151.
E-mail address: yele.gopi@gmail.com (V. Gopinath).
Peer review under responsibility of King Saud University.

Production and hosting by Elsevier

http://dx.doi.org/10.1016/j.arabjc.2016.02.005

viability of GNP7 and GNP55 on AGS cell lines showed no toxicity at the MIC of *H. pylori*. The biogenic GNP has excellent biocompatibility, anti-*H. pylori* and catalytic properties of multifaceted biomedical applications.

1. Introduction

Gold nanoparticles have been synthesized for more than three centuries ago due to their fascinating optical characteristics and surface plasma resonance (SPR) mediated color development. Owing to their physical and chemical properties, they are applicable in electrochemistry, optoelectronics, biomedicine, biochemical sensing, catalysis, chemical stability and biolabeling (Dreaden et al., 2012; MubarakAli et al., 2013). Recently metal nanoparticles are attempting to improve novel methods for reducing nitro compounds, which display non-toxic or less toxicity (Anand et al., 2015). GNP is also known to have disinfecting effects and has been used in many applications ranging from traditional medicines to culinary items. Several salts of gold, silver and their derivatives are commercially manufactured as antimicrobial agents (Krutyakov et al., 2008). At low concentrations, GNP is safe to human cells, but lethal for bacteria and viruses and induces cellular damage by various pathways resulting in difficulty for bacteria to attain resistance against them (MubarakAli et al., 2011; Mishra et al., 2011; Cui et al., 2012).

It has been reported that GNPs functionalized with chitosan and liposomes are highly stable in gastric acid, and capable of fusing with bacteria at physiological pH, making them suitable to treat gastric pathogens such as *Helicobacter pylori* infections (Thamphiwatana et al., 2014). Previously few studies have been carried out to explore the involvement of reactive oxygen species (ROS) mediated DNA damage by exposure to GNP in different cell types (Khiang et al., 2012). Several studies reported that GNPs cause cellular damage to mammalian cells through unintended mechanisms including induction of necrosis and apoptosis (Pan et al., 2007; Leite et al., 2015), oxidative stress, inflammation, DNA damage and alterations in gene expression (Li et al., 2010). However, there are some contradictory reports on non-toxicity of GNPs to various mammalian cells under ambient conditions. Moreover, there is limited report on GNP toxicity on gastric cell lines, where *H. pylori* predominately cause peptic ulcers in immune-compromised patients. In addition, shape and functionalization are the factors for cellular uptake, membrane interaction and cellular toxicity (Schaeublin et al., 2012; Oh et al., 2011).

The synthesis of nanoparticles using microorganisms or different parts of plants can potentially eliminate these problems by making nanoparticles more biocompatible. In recent years, synthesis of gold nanoparticles has been widely reported with various plant materials such as *Lantana montevidensis* and *Solanum lycopersicum* (Mukherjee et al., 2015; Raliya et al., 2015). Unlike, various physical and chemical approaches are available to synthesize AuNPs, while almost all those methods are energy or capital intensive (Shi et al., 2015). This study focused on the synthesis of GNPs using extract of dried fruits of *Tribulus terrestris*. These synthesized GNPs were analytically investigated for their biomolecular interaction, shape and sizes. To understand the biocompatibility of GNPs cytotoxicity was performed on AGS cell lines, and size dependent anti-*H. pylori* activity was also investigated for the GNPs. In addition, catalytic property of GNP was examined to reduce a toxic, *p*-nitroaniline to *p*-phenylenediamine to a non-toxic by-product. These compiled reports could prove the multifaceted potentials of GNPs for utilization in targeted ulcer treatment and scavenging toxicants.

2. Materials and methods

2.1. Chemicals and plant materials

All the chemicals and media were procured from Sigma Aldrich (St. Louis, USA). The dried fruit materials of *T. terrestris* were purchased from local market in Chennai, India. Double sterilized deionized water was used throughout the experiments.

2.2. Bacterial and cell culture

The multi-drug resistant *H. pylori* strains, UM37, UM38, UM67, UM77, UM119 and UM158, were obtained from Helicobacter Research Laboratory, University of Malaya, Kuala Lumpur, Malaysia. The antibiotic sensitivity test of these strains was extensively studied by our laboratory (Teh et al., 2014). Gastric adenocarcinoma AGS cells (ATCC 43504) were procured from American Type Culture Collection (ATCC, USA).

2.3. Preparation of plant extract and GNPs

The dried fruits of *T. terrestris* were rinsed twice with Milli-Q water to remove the dust materials and were dried under direct sunlight for 7 days to complete removal of moisture. The dried fruits pulverized well with mortar and pestle to form powder (Gopinath et al., 2012, 2015). Three gram of sample was mixed into 100 mL of deionized water and boiled for 10 min in order to enhance the phytochemicals in the extract. The fruit extract was filtered through 0.2 μm Millipore filter after warm down. 100 mL of filtrate was mixed with $HAuCl_4$ to achieve the final volume concentration of 1 mM and 2 mM solution with constant stirring. The color change was periodically observed.

2.4. Physico-chemical characterization of GNP

The GNPs were primarily characterized by UV–Vis spectroscopy (UV–Vis: N06354, Thermo Fisher, Finland) gauzed in the range of 200–700 nm, at a resolution of 1 nm. IR spectral analysis was performed to fruit extract as well as the biogenic GNP using fourier transform infrared spectroscopy (FTIR: Cary 660, Agilent technologies, USA) and spectra were recorded at a resolution of 4 cm^{-1} at the range of 500–4000 cm^{-1}. The crystallinity of the GNPs was studied by X-ray diffractometer (XRD: PANalytical XpertPro, the Netherlands) operated at a voltage of 40 keV in the scan ranges of 20–80°. Size and shape of GNPs were investigated by HRTEM (HRTEM: JSM- JEOL 2100, Japan) equipped with EDAX for an elemental analysis.

Please cite this article in press as: Gopinath, V. et al., Anti-*Helicobacter pylori*, cytotoxicity and catalytic activity of biosynthesized gold nanoparticles: Multifaceted application. Arabian Journal of Chemistry (2016), http://dx.doi.org/10.1016/j.arabjc.2016.02.005

2.5. Antibacterial assay of selected GNPs against H. pylori strains

2.5.1. Disk diffusion assay

The antibacterial assay was performed against multi-drug resistant bacterial strains of *H. pylori*. The selected strains of *H. pylori* grown up to 72 h to obtain the concentration of 1×10^5 CFU were inoculated on chocolate agar medium (Oxoid, UK) supplemented with 7% of lysed horse blood. The selected GNP7 and GNP55 were loaded in sterile disks with 6 mm dimension at the concentration of 5, 10, 15, 20 μg/mL. The plates were incubated at 37 °C for three days in a humidified 10% CO_2 incubator at 37 °C. The clear zones of inhibition around the disks were observed and measured. The disk loaded with the fruit extract served as a control for this experiment.

2.5.2. Determination of the minimum inhibitory concentration (MIC)

To determine MIC of GNP7 and GNP55, a standard of Clinical and Laboratory Standards Institute (CLSI) broth microdilution method was followed. Briefly, the test strains were subcultured in appropriate conditions mentioned previously. The cultures were then adjusted to 0.5 Mcfarland standards to obtain 50 μL, $\sim 10^8$ CFU/mL. Broth was dispensed into the wells followed by addition of AuNPs solution and inoculum. Serial dilution was performed by addition of various quantities of AuNPs to the 96-well microtitre plate with BHI to reach the concentration 2.5–50 μg/mL. The microtitre plate wells containing the brain heart infusion (BHI) fresh medium served as a negative control and the wells containing bacterial suspension served as a positive control. MIC_{50} was determined as the lowest concentration of the GNP that reduces growth by above 50%. The bacterial content in the plate showing no visible growth was sub-cultured on chocolate agar plates supplemented with 7% lysed horse blood and incubated at 37 °C for 72 h. After incubation period the plates showing no visible growth were considered as Minimum bactericidal concentration (MBC_{99}). The highest dilution showing at least 99% of reduction in growth was considered as MBC.

2.6. Cell viability assay by Annexin-V/Propidium Iodide (PI) staining

Biocompatibility of GNPs was studied with human adenocarcinoma AGS cell lines and confirmed by Annexin V- Alexa Flour 488 and Propidium Iodide (PI) staining (Tali apoptosis kit, USA). The AGS cells were treated with GNP7 and GNP55 at the concentrations of 2.5–200 μg/mL for 8, 16 and 24 h. Untreated cells were served as a positive control for viable cells, while Staurosporine treated cells were served as a positive control for dead cells. Thereafter, the cells were centrifuged at 3000*g* for 5 min and the pellet was suspended with binding buffer followed by stained with Annexin-V and kept stand for 20 min under dark condition. Finally, cells were then centrifuged at 3000*g* for 5 min and suspended the pellet with binding buffer followed by PI for 5 min in dark at 37 °C. The cells were stained with Annexin V/PI loaded into the slide chamber through capillary action and the slide was analyzed by Tali Image-based Cytometer. The slide was observed under a FLoid Cell Imaging station (Molecular probes life technologies, USA) as per the manufacturer's instructions.

2.7. Reduction of p-nitroaniline by GNPs

In a typical catalytic reaction, reduction of nitroaromatic compounds was induced by the addition of GNP7 and GNP55 to assess their size dependent activity. The freshly prepared 10 mM $NaBH_4$ aqueous solution was mixed with 1 mM and 10 mM *p-nitroaniline* (4-NA) solution separately. The colloidal GNP7 and GNP55 were then added to the above reaction mixture to enhance the rate of reduction reaction. The reduction of 4-NA to 4-PDA (*p*-phenylenediamine) was monitored by spectrophotometrically in ambient condition.

3. Results and discussion

3.1. Synthesis and optimization of GNPs

An eco-friendly way one-pot generation of viable and multifaceted GNPs was successfully synthesized using dried fruit extract of *T. terrestris*. GNPs were generated when 1 mM and 2 mM of $HAuCl_4$ were mixed with filtered extract. The ionic (Au^+) was reduced into metallic (Au^0) GNP and it was periodically confirmed by the color changes. The color of the solution turned pale yellow to ruby-red which confirms the SPR of GNPs. The intensity of the color was gradually increased to saturation as a function of time (6, 8, 10 and 12 h) in both the reaction mixtures (1 and 2 mM) Insight (Fig. 1a and b). UV–Vis spectra showed gradual increase in peak intensity at 500–550 nm which demonstrated that the growth and formation of GNP, which confirms an increase in the concentration of the metal ions showed increase in particle size and no significant sharp peak was found at higher metal concentration in visible or NIR region. The spectra showed the strong peak at 540 nm after 12 h of incubation which was the remarkable characteristic of GNPs (Kumar et al., 2008, 2011; Dubey et al., 2010). The *T. terrestris* fruit extract alone used as a control showed a peak at 280 nm. It could be due to the functional biomolecules present in the fruit extract (Gopinath et al., 2012).

3.2. Physico-chemical analysis of GNPs

The possible biomolecules responsible for the reduction were confirmed by FTIR spectrum and understanding the interaction of GNPs and biomolecules, and this study focused only to GNP55 (Fig. 2) showed the intense peak at 1645 cm^{-1} which corresponds to the (C═O) NH_2 carbonyl stretching amide functional group; the peak at 2137 cm^{-1} was identified as C—C stretching vibrations and the peak at 745 cm^{-1} was arisen due to the O—C stretching vibrations of protein present in the dried fruit extract (Gopinath et al., 2013; Dwivedi et al., 2010; Saravanan et al., 2011). The IR spectrum of extract reduced GNP showed the bands at 3390, 2136, 1642 and 741 cm^{-1} (Fig. 2b). There was slight shift absorbed in the peak position as well as the wavelength. Due to the formation of GNP the major shift was observed in the peak position from 3406 to 3390 cm^{-1} which is the characteristic of OH stretching vibrations (Gopinath and velusamy, 2013). The preliminary IR

Please cite this article in press as: Gopinath, V. et al., Anti-*Helicobacter pylori*, cytotoxicity and catalytic activity of biosynthesized gold nanoparticles: Multifaceted application. Arabian Journal of Chemistry (2016), http://dx.doi.org/10.1016/j.arabjc.2016.02.005

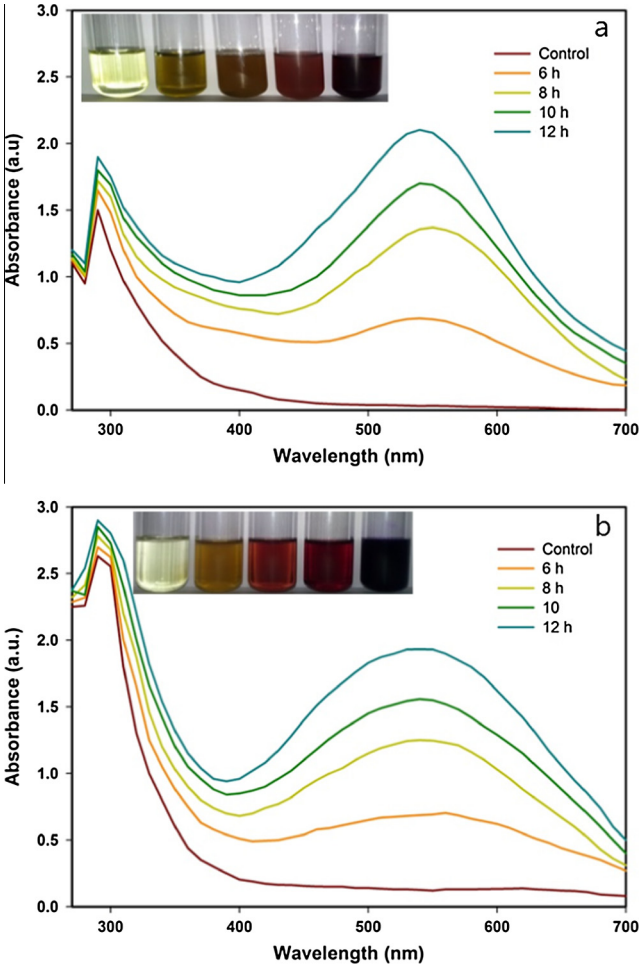

Figure 1 UV–Visible spectra of fruit extract mediated generation of GNPs mixed with 1 mM and 2 mM aqueous $HAuCl_4$ (a and b) in various time period (6, 8, 10 and 12 h).

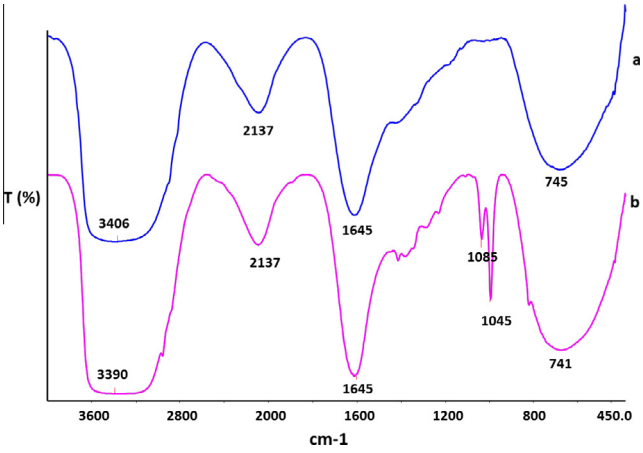

Figure 2 FTIR spectra of *T. terrestris* fruit extract (a) fruit mediated generation of GNP55 (b).

result suggested that the carbonyl and hydroxyl functional group present in the fruit extract which may be responsible for the bioreduction of GNP.

The crystallinity of GNPs was confirmed using XRD (Fig. 3a). The diffraction peaks at 32.07°, 38.26°, 44.50° and 77.68° corresponded to the (111), (200), (220) and (311) planes of the cubic phase suggest that GNPs are crystalline in nature and the peaks were matched with the JCPDS file no. 00-004-0784 (Kasthuri et al., 2009). The broad peak at the bottom indirectly evidenced the small sized GNP. The elemental analysis spectrum results showed the strong intensity signals of Au which indicated the formation of GNP (Fig. 3b). The observed signal for Al was due to the aluminium foil on which the nanoparticle samples were loaded for analysis (Gopinath et al., 2015).

HRTEM image of the GNPs synthesized using 1 and 2 mM $HAuCL_4$ using *T. terrestris* fruit extract is shown in Fig. 4a and b. In both the experiments, distinct particles and most of the particles are spherical (1 mM), but a few triangular were also observed (2 mM) and the average size of the GNP was 7 nm and 55 nm respectively. The particle size was increased as the concentration of $HAuCL_4$ increased to 2 mM. Moreover most of the particles' multifaceted structures had triangular, spherical, hexagonal and truncated shapes. GNPs usually formed spherical to triangular shaped particles have also been prepared by plant extract mediated synthesis with larger diameters around 5–300 nm (Kuo et al., 2004; Song et al., 2009; MubarakAli et al., 2013).

3.3. Size dependent anti-*H. pylori* activity of GNPs

Anti-*H. pylori* property of GNPs was determined and clear zones of inhibitions were observed around disks loaded with GNP7 and GNP55, which clearly confirms the antibacterial

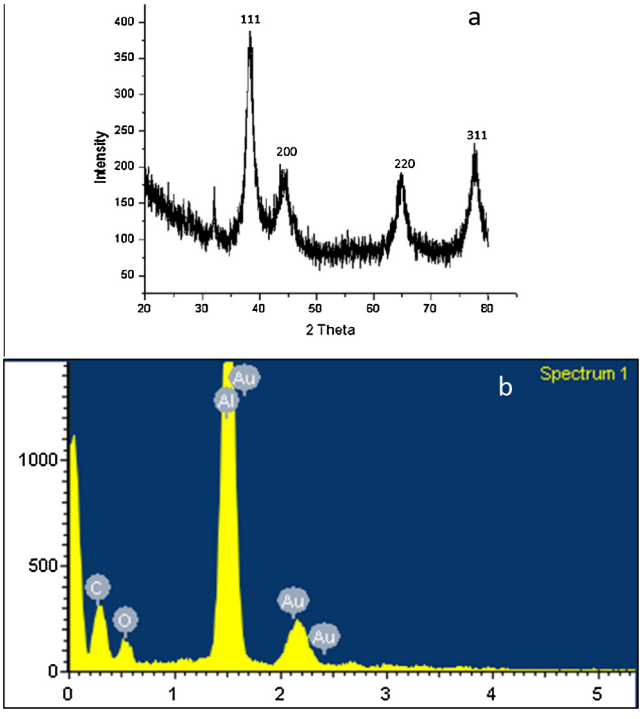

Figure 3 XRD pattern of GNPs (a) showed crystalline nature of GNPs with (111), (200), (220): (ICDD file no. 00-004-0784); (b) EDAX spectrum of GNPs.

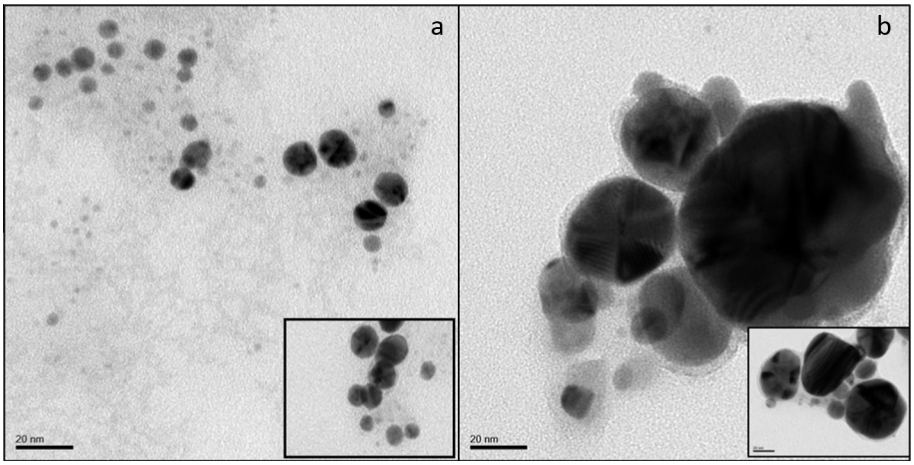

Figure 4 HRTEM images of GNP: (a) the spherical shaped at the average size of 7 nm (GNP7) and (b) anisotropic particles at the average size of 55 nm (GNP55).

effect of GNPs. Interestingly, GNP55 showed more effective against *H. pylori* than GNP7 upon various concentrations (Table 1). The antibacterial efficacy of GNPs was increased as the size of the GNPs was increased. *H. pylori* UM119 showed susceptible (12.1 mm) to GNP55 at high concentration of 20 μg/mL whereas *H. pylori* UM037 showed resistance (10.5 mm) to GNP55 at the same concentration. It could be due to different mechanisms of metal resistance among different strains. The present investigation clearly indicated the size dependent anti-*H. pylori* activity of GNP among tested *H. pylori* strains. The permeability of the cell membrane increased significantly with exposure to increase in the size and concentration of GNPs (Badwaik et al., 2012). MIC of GNP tested for their *in vitro* anti-*H. pylori* activity revealed that GNP55 inhibits the bacterial growth relatively at low concentration than the GNP7 at 16.75 μg/mL of GNP55 and 18 μg/mL of GNP7 for *H. pylori* UM158 and other strains are shown (Table 2). MBC of GNP revealed bactericidal effect of GNP55 at 18.75 μg/mL of GNP55 and 20.50 μg/mL of GNP7 for *H. pylori* UM038. The GNPs are effective against *H. pylori* reflecting that GNP could be used as potent anti-*H. pylori* agents. The lowest concentration is much more applicable for therapeutic applications for *H. pylori* (Mollick et al., 2014).

Table 1 Anti-*Helicobacter pylori* activity of GNP7 and GNP55 by agar diffusion assay with various concentrations (5, 10, 15 and 20 μg/mL).

S. No.	Strains	Concentration of GNP (μg/ml)	Zone of inhibition (mm)	
			GNP7	GNP55
1	*H. pylori* UM037	5	0.0	0.0
		10	6.9	7.1
		15	9.2	9.2
		20	10.2	10.4
2	*H. pylori* UM038	5	0.0	0.0
		10	7.2	7.5
		15	9.5	9.8
		20	11.0	11.5
3	*H. pylori* UM067	5	0	0.0
		10	7.8	7.8
		15	9.0	9.3
		20	11.6	11.9
4	H. pylori UM077	5	0.0	0.0
		10	7.6	8.0
		15	9.2	9.5
		20	11.3	11.8
5	*H. pylori* UM119	5	0.0	0.0
		10	7.9	8.2
		15	9.6	9.7
		20	11.8	12.1
6	*H. pylori* UM158	5	0.0	0.0
		10	7.4	7.7
		15	9.7	10.0
		20	11.5	11.9

3.4. Biocompatibility of GNP7 and GNP55

The rate of cell proliferation was estimated with AGS cell lines treated with GNP7 and GNP55 at gradual increased concentration (0–200 μg/mL) at different time periods (8, 16, 24 h)

Table 2 MIC and MBC of GNP7 and GNP55 against various strains of *H. pylori*.

S. No.	Strains	MIC (μg/ml)		MBC (μg/ml)	
		GNP7	GNP55	GNP7	GNP55
1	*H. pylori* UM037	19.00	17.00	22.75	20.50
2	*H. pylori* UM038	16.75	16.00	20.50	18.75
3	*H. pylori* UM067	18.50	18.00	23.75	22.00
4	*H. pylori* UM077	21.50	20.00	24.50	23.00
5	*H. pylori* UM119	21.00	19.25	23.75	22.50
6	*H. pylori* UM158	18.00	16.75	21.75	19.25

Please cite this article in press as: Gopinath, V. et al., Anti-*Helicobacter pylori*, cytotoxicity and catalytic activity of biosynthesized gold nanoparticles: Multifaceted application. Arabian Journal of Chemistry (2016), http://dx.doi.org/10.1016/j.arabjc.2016.02.005

and the cells were stained with Annexin V and PI. The cells treated with GNP7 at 200 μg/mL showed significantly high rate of anti-proliferative than that of GNP55 at 11.33%, 17.33% and 28.66% respective of treatment time at 8, 16 and 24 h (Fig. 5a). It is noteworthy to mention that the anti-proliferative of GNP55 was found to be lower at the highest concentration such as 10%, 15.6% and 25.6% exposed to 8, 16 and 24 h respectively (Fig. 5b). Interestingly, GNPs concentration at 50 μg/mL showed non-toxic level. The MIC of all the strains showed the maximum of 21.5 μg/mL. Therefore, biogenic GNPs not affected AGS cells at these concentrations are effective to *H. pylori*. It has recently been reported that the cellular uptake of nanoparticles ranging from 15 to 100 nm depends on size (Jiang et al., 2008; Wang, 2011). The cytotoxicity of GNPs depended primarily on their size such as 1–2 nm was highly toxic and more than 15 nm was comparatively non-toxic, irrespective of the cell against epi and endothelial, phagocytes and tissue stromal cells (Pan et al., 2007). This study confirmed that AGS cells treated with GNP55 have minimally lower percentage of apoptotic cell death compared to the GNP7.

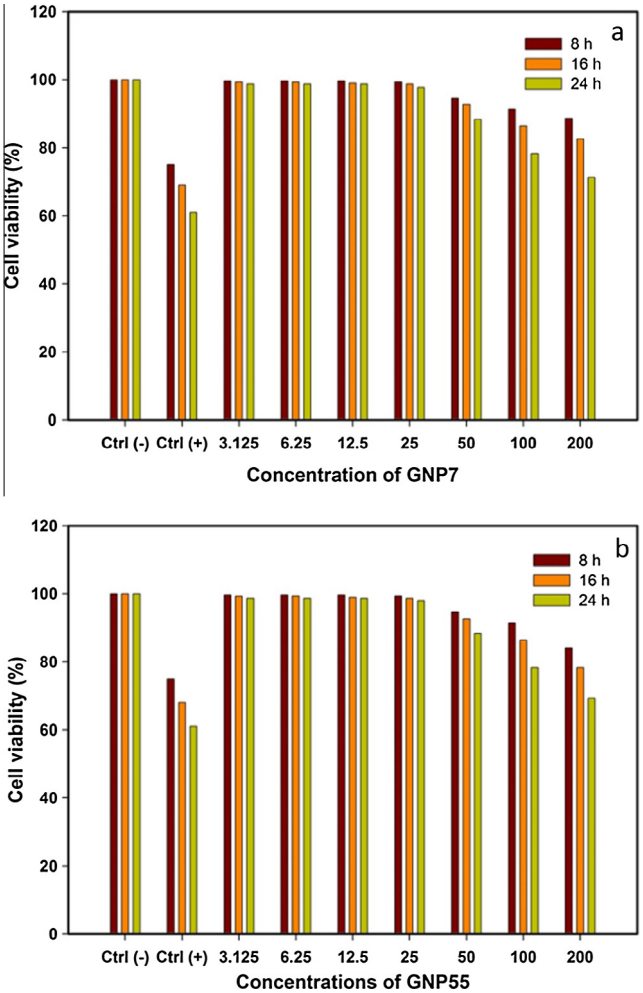

Figure 5 Cell viability of GNPs using Tali cytometry analysis against AGS cell lines (a and b). The cells were stained with propidium iodide and annexin-V after 8, 16 and 24 h treatment with GNP7 and GNP55.

3.5. Catalytic activity of GNP7 and GNP55

The biogenic GNPs showed size dependent catalytic reduction of *p-nitroaniline* was monitored by UV–Vis spectroscopic analysis. The rate of reduction of *p*-nitroaniline to *p*-phenylenediamine was increased with $NaBH_4$ in aqueous GNPs. The GNP7 and GNP55 were mixed with 4-NA in the presence of $NaBH_4$ medium showed sustainable decrease in absorbance at 380 nm shifted to 220 nm and formation of a new peak at 305 nm as of incubation period for 0–56 min in GNP7 (Fig. 6a) and 0–72 min in GNP55 (Fig. 6b). The reduction reaction was completed at 56 min using GNP7 as a catalyst, and it was relatively lower at 72 min when GNP55 was used. The control experiment of 4-NA reduction with $NaBH_4$ after 24 h showed slight change in the peak position at 380 nm which is the characteristic for 4-NA. The schematic representation of *p*-nitroaniline reduction is presented in Fig. 7.

Among environmental and genotoxic pollutants, nitroaromatic compounds (NAC) such as *p-nitroaniline* were considered to be toxic and exhibit serious carcinogenic and mutagenic effects (Singh et al., 2014). NAC reduction with an excess amount of $NaBH_4$ has often been used as a model reaction. For instance, the catalysis of *p*-nitroaniline reduction

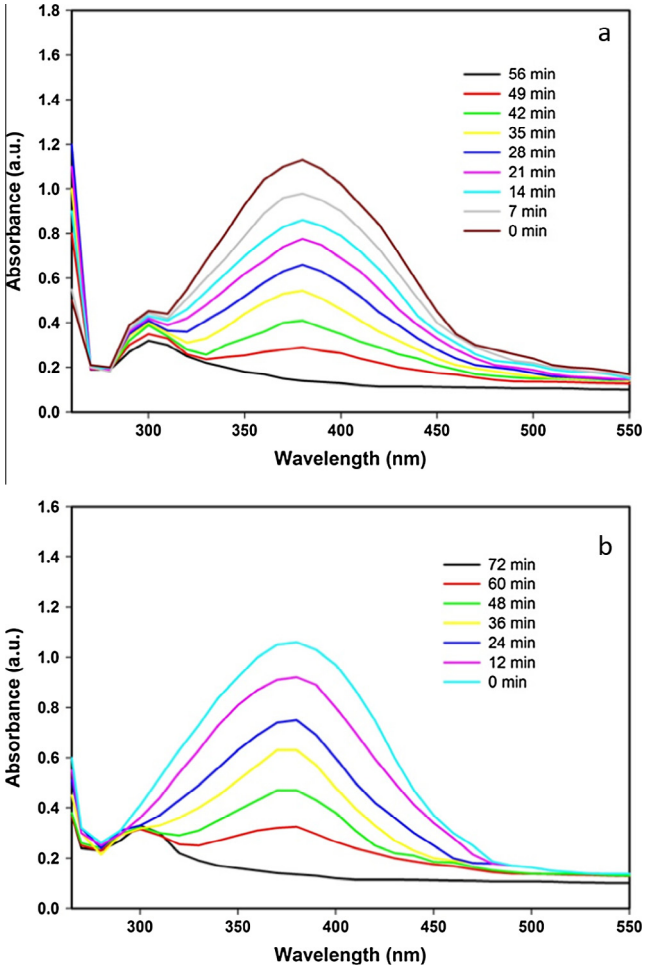

Figure 6 Catalytic reduction of *p*-nitroaniline with $NaBH_4$ by biogenic GNP7 and GNP55 synthesized from 1 mM (a) and 2 mM (b) of $HAuCl_4$.

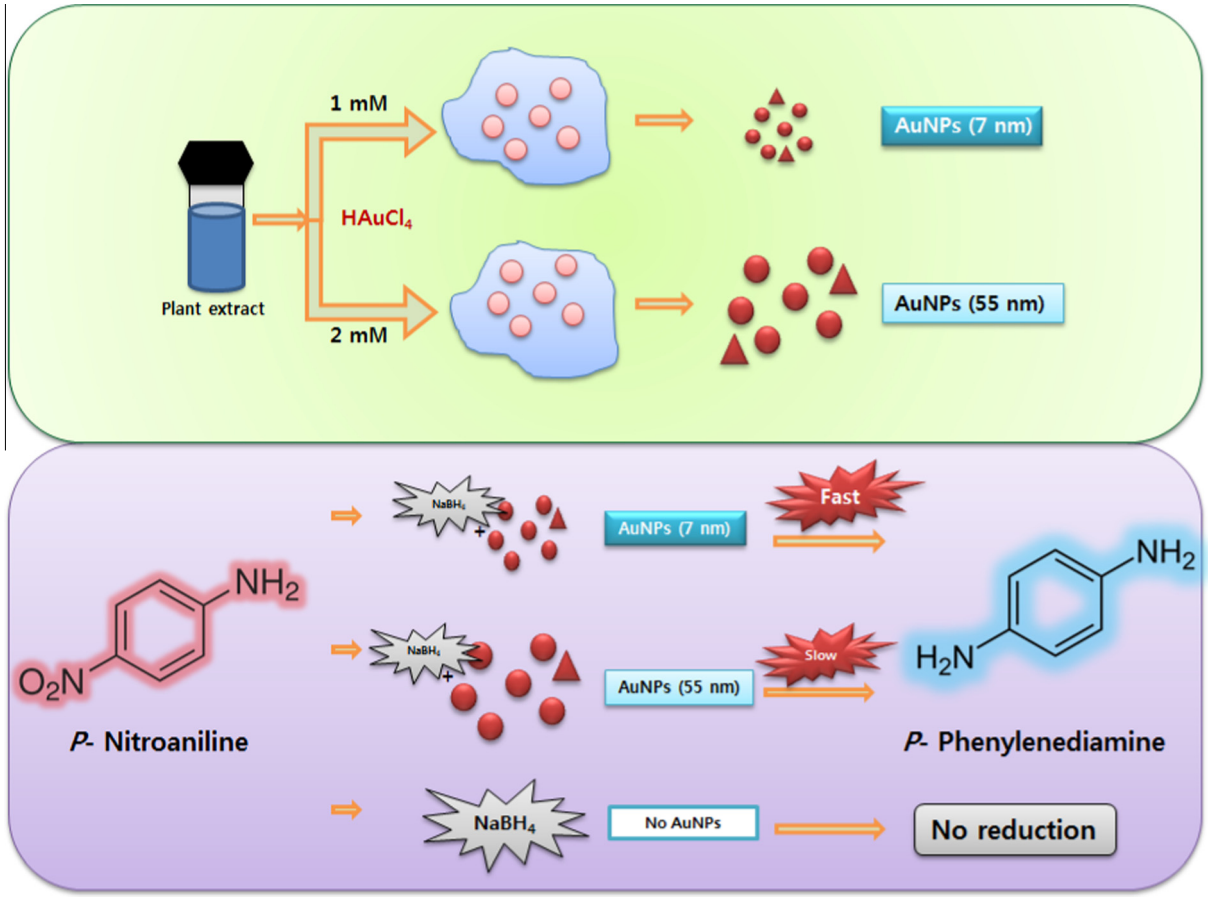

Figure 7 Schematic diagram of the size dependent catalytic activity of GNPs by the reduction of *p*-nitroaniline in the presence of $NaBH_4$.

of GNP with the presence of $NaBH_4$ was reported (Shi et al., 2015). This study light up the plant synthesized GNPs was accelerating the reduction of *p*-nitroaniline to *p*-phenylenediamine in the presence of $NaBH_4$. The product of this chemical reduction, *p*-phenylenediamine, is an attractive intermediate in the preparation of polymers, hair dyes, and rubber products (Hsiao-Shu et al., 2011). In this study, it was found that antibacterial and catalytic activity strongly correlates with sizes of the GNPs.

4. Conclusions

To summarize, a one pot method of green synthesis of GNPs was reported using *T. terrestris* fruit extract. Different sized GNPs were synthesized using 1 mM and 2 mM of $HAuCl_4$. Interaction of biomolecules with GNPs analyzed that C═O and OH─ functional groups present in the extract could be a reducing and capping agent for GNPs. Anisotropic GNPs were synthesized with average size of 7 nm and 55 nm in ambient conditions. Both GNP7 and GNP55 exhibited anti-*H. pylori* activity against multi-drug resistant clinical strains of *H. pylori*. MIC of GNP7 and GNP55 did not show cytotoxic effect against AGS cells. Furthermore, GNPs showed size-dependent catalytic activity of reducing a toxic *p*-nitroaniline. These results support the development of a novel anti-*H. pylori* drug using simple route synthesized GNPs.

Funding

This research was supported by High Impact Research Chancellery Grant UM.C/625/1/HIR/MoE/CHAN/13/2 (Account No. H-50001-A000032) from the University of Malaya-Ministry of Education, Malaysia.

Acknowledgement

The authors would like to thank Deanship of Scientific Research, College of Science Research Centre, King Saud University, Kingdom of Saudi Arabia.

References

Anand, K., Gengan, R.M., Phulukdaree, A., Chuturgoon, A., 2015. Agroforestry waste *Moringa oleifera* petals mediated green synthesis of gold nanoparticles and their anti-cancer and catalytic activity. J. Indus. Eng. Chem. 21, 1105–1111.

Badwaik, V.D., Vangala, L.M., Pender, D.S., Willis, C.B., Aguilar, Z. P., Gonzalez, M.S., Paripelly, R., Dakshinamurthy, R., 2012. Size-dependent antimicrobial properties of sugar-encapsulated gold nanoparticles synthesized by a green method. Nanosc. Res. Lett. 7 (1), 623.

Cui, Y., Zhao, Y., Tian, Y., Zhang, W., Lüa, X., Jiang, X., 2012. The molecular mechanism of action of bactericidal gold nanoparticles on *Escherichia coli*. Biomaterials 33 (7), 327–2333.

Dreaden, E.C., Alkilany, A.M., Huang, X., Murphy, C.J., El-Sayed, M.A., 2012. The golden age: gold nanoparticles for biomedicine. Chem. Soc. Rev. 41, 2740–2779.

Dubey, S.P., Lahtinen, M., Sarkka, H., Sillanpaa, M., 2010. Bio-prospective of *Sorbus aucuparia* leaf extract in development of silver and gold nanocolloids. Colloids Surf. B 80, 26–33.

Dwivedi, A.D., Gopal, K., 2010. Biosynthesis of silver and gold nanoparticles using *Chenopodium album* leaf extract. Colloids Surf. A 369, 27–33.

Gopinath, V., MubarakAli, D., Priyadarshini, S., Meera Priyadarshini, N., Thajuddin, N., Velusamy, P., 2012. Biosynthesis of silver nanoparticles from *Tribulus terrestris* and its antimicrobial activity: a novel biological approach. Colloids Surf. B 96, 69–74.

Gopinath, V., Priyadarshini, S., Loke, M.F., Arunkumar, J., Marsili, E., MubarakAli, D., Velusamy, P., Vadivelu, J., 2015a. Biogenic synthesis, characterization of antibacterial silver nanoparticles and its cell cytotoxicity. Arab. J. Chem. http://dx.doi.org/10.1016/j.arabjc.2015.11.011.

Gopinath, V., Priyadarshini, S., Priyadharshini, N.M., Pandian, K., Velusamy, P., 2013. Biogenic synthesis of antibacterial silver chloride nanoparticles using leaf extracts of *Cissus quadrangularis* Linn. Mater Lett. 91, 224–227.

Gopinath, V., Priyadarshini, S., Venkatkumar, G., Saravanan, M., MubarakAli, D., 2015b. *Tribulus terrestris* leaf mediated biosynthesis of stable antibacterial silver nanoparticles. Pharm. Nanotechnol. 3 (1), 26–34.

Gopinath, V., Velusamy, P., 2013. Extracellular biosynthesis of silver nanoparticles using Bacillus sp. GP-23 and evaluation of their antifungal activity towards *Fusarium oxysporum*. Spectrochim. Acta A 106, 170–174.

Hsiao-Shu, L., Yu-Wen, L., 2011. Permeation of hair dye ingredients, p-phenylenediamine and aminophenol isomers, through protective gloves. Ann. Occup. Hyg. 53, 289–296.

Jiang, W., Kim, B.Y.S., Rutka, J.T., Chan, W.C.W., 2008. Nanoparticle-mediated cellular response is size-dependent. Nat. Nanotechnol. 3, 145–150.

Kasthuri, J., Veerapandian, S., Rajendiran, N., 2009. Biological synthesis of silver and gold nanoparticles using apiin as reducing agent. Colloids Surf. B 68, 55–60.

Khiang Oo, M.K., Yang, Y., Hu, Y., Gomez, M., Du, H., Wang, H., 2012. Gold nanoparticle-enhanced and size-dependent generation of reactive oxygen species from protoporphyrin IX. ACS Nano. 6, 1939–1947.

Krutyakov, Y.A., Kudrynskiy, A.A., Olenin, A.Y., Lisichkin, G.V., 2008. Extracellur biosynthesis and antimicrobial activity of silver nanoparticles. Russ. Chem. Rev. 77, 233–257.

Kumar, K.P., Paul, W., Sharma, C.P., 2011. Green synthesis of gold nanoparticles with *Zingiber officinale* extract: characterization and blood compatibility. Proc. Biochem. 46, 2007–2013.

Kumar, S.A., Peter, Y.A., Nadeau, J.L., 2008. Facile biosynthesis, separation and conjugation of gold nanoparticles to doxorubicin. Nanotechnology 19, 495101–495111.

Kuo, C.H., Chiang, T.F., Chen, L.J., Huang, M.H., 2004. Synthesis of highly faceted pentagonal- and hexagonal-shaped gold nanoparticles with controlled sizes by sodium dodecyl sulfate. Langmuir 20, 7820–7824.

Leite, P.E.C., Pereira, M.R., Santos, C.A.N., Campos, A.P.C., Esteves, T.M., Granjeiro, J.M., 2015. Gold nanoparticles do not induce myotube cytotoxicity but increase the susceptibility to cell death. Toxicol. In Vitro. 29, 819–827.

Li, J.J., Hartono, D., Ong, C.N., Bay, B.H., Yung, L.Y., 2010. Autophagy and oxidative stress associated with gold nanoparticles. Biomaterials 31, 5996–6003.

Mishra, A., Tripathy, S.K., Yun, S., 2011. Bio-synthesis of gold and silver nanoparticles from *Candida guilliermondii* and their antimicrobial effect against pathogenic bacteria. J. Nanosci. Nanotechnol. 11, 243–248.

Mollick, M.R., Bhowmick, B., Mondal, D., Maity, D., Rana, D., Dash, S.K., Chattopadhyay, S., Roy, S., Sarkar, J., Acharya, K., Chakrabortye, M., Chattopadhyay, D., 2014. Anticancer (in vitro) and antimicrobial effect of gold nanoparticles synthesized using Abelmoschus esculentus (L.) pulp extract via a green route. RSC Adv. 4, 37838.

MubarakAli, D., Arunkumar, J., Harish Nag, K., SheikSyedIshack, K.A., Baldev, E., Pandiaraj, D., Thajuddin, N., 2013. Gold nanoparticles from Pro and eukaryotic photosynthetic microorganisms comparative studies on synthesis and its application on biolabelling. Colloids Surf. B 103, 166–173.

MubarakAli, D., Thajuddin, N., Jeganathan, K., Gunasekaran, M., 2011. Plant extract mediated synthesis of silver and gold nanoparticles and its antibacterial activity against clinically isolated pathogens. Colloids Surf. B 85, 360–365.

Mukherjee, S., Dasari, M., Priyamvada, S., Kotcherlakota, R., Bollu, V.S., Patra, C.R., 2015. A green chemistry approach for the synthesis of gold nanoconjugates that induce the inhibition of cancer cell proliferation through induction of oxidative stress and their in vivo toxicity study. J. Mater. Chem. B 3, 3820.

Oh, E., Delehanty, J.B., Sapsford, K.E., Susumu, K., Goswami, R., Blanco-Canosa, J.B., Dawson, P.E., Granek, J., Shoff, M., Zhang, Q., Goering, P.L., Huston, A., Medintz, I.L., 2011. Cellular uptake and fate of PEGylated gold nanoparticles is dependent on both cell-penetration peptides and particle size. ACS Nano. 5, 6434–6448.

Pan, Y., Neuss, S., Leifert, A., Fischler, M., Wen, F., Simon, U., Schmid, G., Brandau, W., Dechent, W.J., 2007. Size-dependent cytotoxicity of gold nanoparticles. Small 3, 1941–1949.

Raliya, R., Biswas, P., 2015. Environmentally benign bio-inspired synthesis of Au nanoparticles, their self-assembly and agglomeration. RSC Adv. 5, 42081.

Saravanan, M., Vemu, A.K., Barik, S.K., 2011. Rapid biosynthesis of silver nanoparticles from *Bacillus megaterium* (NCIM 2326) and their antibacterial activity on multi drug resistant clinical pathogens. Colloids Surf. B 88, 325–331.

Schaeublin, N.M., Braydich-Stolle, L.K., Maurer, E.I., Park, K., Maccuspie, R.I., Afrooz, A.R., Vaia, R.A., Saleh, N.B., Hussain, S. M., 2012. Does shape matter? Bioeffects of gold nanomaterials in a human skin cell model. Langmuir 28, 3248–3258.

Shi, C., Zhu, N., Cao, Y., Wu, P., 2015. Biosynthesis of gold nanoparticles assisted by the intracellular protein extract of *Pycnoporus sanguineus* and its catalysis in degradation of 4-nitroaniline. Nanosc. Res. Lett. 10, 147.

Singh, C., Goyal, A., Singhal, S., 2014. Nickel-doped cobalt ferrite nanoparticles: efficient catalysts for the reduction of nitroaromatic compounds and photo-oxidative degradation of toxic dyes. Nanoscale 6, 7959–7970.

Song, J.Y., Jang, H.K., Kim, B.S., 2009. Biological synthesis of gold nanoparticles using *Magnolia kokus* and *Diopyros kaki* leaf extracts. Proc. Biochem. 44, 1133–1138.

Teh, X., Khosravi, Y., Lee, W.C., Leow, A.H.R., Loke, M.F., Vadivelu, J., Goh, K.L., 2014. Functional and molecular surveillance of *Helicobacter pylori* antibiotic resistance in Kuala Lumpur. PLoS ONE 9 (7), 101481.

Thamphiwatana, S., Gao, W., Pornpattananangkul, D., Zhang, Q., Fu, V., Li, J., Li, J., Obonyo, M., Zhang, L., 2014. Phospholipase A2-responsive antibiotic delivery via nanoparticle-stabilized liposomes to treat bacterial infection. J. Mater Chem. B 2, 8201–8207.

Wang, H.H., Lin, C.A., Lee, C.H., Lin, Y.C., Tseng, Y.M., Hsieh, C. L., Chen, C.H., Tsai, C.H., Hsieh, C.T., Shen, J.L., Chan, W.H., Chang, W.H., Yeh, H.I., 2011. Fluorescent gold nanoclusters as a biocompatible marker for in vitro and in vivo tracking of endothelial cells. ACS Nano. 5, 4337–4344.